

# Differentiating $\pi$ Interactions by Constructing Concave/Convex Surfaces Using a Bucky Bowl Molecule, Corannulene in Liquid Chromatography

Eisuke Kanao,<sup>†</sup> Takuya Kubo,<sup>\*,†©</sup> Toyohiro Naito,<sup>†</sup> Takatoshi Matsumoto,<sup>‡</sup> Tomoharu Sano,<sup>§</sup> Mingdi Yan,<sup>||©</sup> and Koji Otsuka<sup>†</sup>

Supporting Information

**ABSTRACT:** Convex-concave  $\pi$  conjugated surfaces in hemispherical bucky bowl such as corannulene (Crn) have shown increasing utility in constructing self-assembled new functional materials owing to its unique  $\pi$  electrons and strong dipole. Here, we investigate these specific molecular recognitions on Crn by developing new silica-monolithic capillary columns modified with Crn and evaluating their performance in the separation of different aromatic compounds by liquid chromatography (LC). We synthesized two Crn derivatives and conjugated them onto the surface of a



silica monolith. The first Crn derivative was edge functionalized, which can undergo free inversion of a convex-concave surface. The second Crn derivative was synthesized by modifying the spoke of Crn, which suppresses the convex-concave inversion. Results of LC suggest that each surface showed different shape recognition based on  $\pi$  interaction. Furthermore, the concave surface of Crn showed strong CH $-\pi$  interaction with a planar molecule, coronene, demonstrated by the shifts of the <sup>1</sup>H NMR signals of both Crn and coronene resulting from the multiple interactions between Crn and  $\pi$  electrons in coronene. These results clearly demonstrated the presence of  $CH-\pi$  interactions at multiple points, and the role of shape recognition.

he  $\pi$  interaction is a type of noncovalent interaction with aromatic compounds and plays an important role in the molecular recognition processes in biological systems and organic functional materials. 1-5 For example, Nakagawa et al. revealed an oncogenic promoter recognition mechanism caused by the  $CH-\pi$  interaction between kinase C and indole-V derivatives. Recently, many studies suggest that the  $\pi$ interaction is profoundly involved in photo and electronic behaviors of organic functional materials. Okamoto et al. developed organic transistors based on a laminating  $\pi$ - $\pi$ interaction, which exhibited 10 times higher electron mobility than conventional transistors. Wu et al. developed an organic thin film capable of regulating visible singlet and near-infrared triplet emissive properties by CH $-\pi$  interaction-assisted selfassembly.8 As can be observed by these and many other reports, a deep understanding and the ability to control  $\pi$ interactions will greatly facilitate the development of new functional materials.

The first bowl-shaped  $\pi$ -conjugated molecule, corannulene, known as a "bucky bowl" and first synthesized by Barth and Lawton in 1966,9 has attracted much interest because of its many unique properties including hemispherical structure, 10 large dipole moment, 11 high electron acceptability, 12,13 and bowl to bowl inversion. 14,15 The bucky bowls have been widely used in the synthesis of new functional materials. 16,17 For example, Sygula et al. designed a clip as a fullerene host, in which two bucky bowl units were connected through a rigid benzo cyclooctatetraene linker.<sup>18</sup> Mack et al. synthesized extended bucky bowl  $\pi$ -systems having potential applications as blue emitters in organic light emitting diodes. 19

Generally, it is challenging to study  $\pi$  interactions especially in the presence of other molecular interactions because  $\pi$ interactions are much weaker than most molecular interactions, such as hydrophobic interaction, hydrogen bonding, and electrostatic bonding. Computational approaches to study

Received: November 13, 2018 Accepted: December 24, 2018 Published: December 24, 2018

<sup>&</sup>lt;sup>†</sup>Graduate School of Engineering, Kyoto University, Katsura, Nishikyo-ku, Kyoto 615-8510, Japan

<sup>&</sup>lt;sup>‡</sup>Institute of Multidisciplinary Research for Advanced Materials, Tohoku University, 2-1-1 Katahira, Aoba-ku, Sendai 980-8577, Japan

<sup>§</sup>Center for Environmental Measurement and Analysis, National Institute for Environmental Studies, Onogawa 16-2, Tsukuba, Ibaraki 305-8506, Japan

Department of Chemistry, University of Massachusetts Lowell, One University Avenue, Lowell, Massachusetts 01854, United

Scheme 1. Preparation of the Crn-PFPA Column: (a) Synthesis of Crn-PFPA-CO<sub>2</sub>CH<sub>3</sub> and Crn-PFPA; (b) Surface Modification of a Silica Monolith by Crn-PFPA

molecular interactions using quantum mechanical models have seen much progress in recent years due to the significant improvement in both algorithms and computing power. ^{20-23} Also, nuclear magnetic resonance (NMR) spectroscopy has been successfully applied to study strong molecular interactions such as H bonding. ^24-27 In this study, we suggest a further straightforward experimental method to measure the strength of  $\pi$  interactions and estimate the interaction mechanism, and then the computational study and spectroscopic approaches will be more reliable.

High performance liquid chromatography (HPLC) is a powerful separation technique that is able to distinguish the partition coefficients of solutes between the mobile and stationary phases and can sensitively reflect the strength of molecular interactions. <sup>28,29</sup> In our previous studies, we successfully immobilized  $C_{60}$ -fullerene (C60) and  $C_{70}$ -fullerene (C70) onto a silica-monolithic capillary and evaluated the characteristics of  $\pi$  interactions of fullerenes. <sup>30–34</sup> In these studies, we succeeded in separating several polycyclic aromatic hydrocarbons (PAHs) by the effective  $\pi-\pi$  interactions. We also showed that fullerenes exhibited specific  $\pi-\pi$  interaction with corannulene resulting from the hemispherical recognition and induced dipole of fullerenes.

In this study, we developed new Crn-coated silica monoliths for the precise understanding of  $\pi$  interactions on the curved  $\pi$ -conjugated surface using LC. Crn is known to have convex and concave surfaces, 35,36 which is expected to lead to different molecular recognition at each surface. Toward this end, we developed two kinds of Crn-functionalized silica monoliths, namely Crn-ester column and Crn-PFPA (perfluorophenyl

azide) columns. The Crn-ester column was prepared from a Crn derivative that was edge functionalized with a -CH<sub>2</sub>OH group, which was then conjugated to a carboxy-functionalized silica monolith. It was anticipated that both surfaces of the Crn structure could interact with solutes<sup>37</sup> in the Crn-ester column. The Crn-PFPA column was prepared from a Crn derivative that was functionalized with PFPA to form an azridine on a spoke of Crn.<sup>38</sup> In this case, the aziridine formation converts two sp<sup>2</sup> hybridized carbon atoms of corannulene into pyramidal sp<sup>3</sup> centers, and it breaks the possibility of inversion of convex-concave surface. Using these two new columns, we evaluated the strength of  $\pi$  interactions between Crn and several PAHs by normal phase liquid chromatography (NPLC), in which hydrophobic interaction was completely reduced and thus  $\pi$  interaction could be examined.<sup>33</sup> To further understand the  $\pi$ - $\pi$  interactions between Crn structure on the stationary phase and Crn as a solute, computational simulations were carried out. In addition, <sup>1</sup>H NMR spectroscopy was employed to examine the interaction between Crn and coronene in detail. This represents the first report that evaluates the shape-based specific interactions on  $\pi$ -conjugated hemispherical surface and multiple  $CH-\pi$  interactions in bucky bowls.

### EXPERIMENTAL SECTION

**Synthesis and Instruments.** We synthesized Crn derivatives and prepared Crn-modified monolithic capillaries as shown in Scheme 1, and Supporting Information, Scheme S1. The detailed experimental procedures and results are summarized in the Supporting Information. Our capillary

liquid chromatographic system consists of a DiNa S (Kya Technologies Co., Tokyo, Japan) as the pump, CE-2070 (Jasco, Tokyo, Japan) as the UV detector, Cheminert (Valco Instruments Co., Huston, TX) as the sample injector, and Chemco capillary column conditioner model 380-b (Chemco Co. Osaka, Japan) as the column oven. The HPLC system is a Prominence series (Shimadzu Co., Kyoto, Japan). FT-IR, NMR, elemental analysis, and direct analysis in real-tyime mass spectroscopy (DARTMS) were carried out on a Nicolet iSS ATR (Thermo Fisher Scientific Inc., Waltham, MA, USA), JNM-ECA500 spectrometer (JEOL, Tokyo, Japan), Flash EA1112 (Thermo Fisher Scientific), and DART (JEOL), respectively.

Surface Modification of the Silica Monolith with Crn-PFPA-NHS. The silica-monolithic capillary was treated with 1.0 M aqueous HCl at 40 °C for 3 h and washed with water and methanol. It was then filled with APTMS in methanol (10%, v/v), remained at room temperature for 24 h, and then washed with methanol to give NH2-modified silica monolith. A solution of Crn-PFPA-NHS in toluene (1.0 mg mL<sup>-1</sup>) was charged into the NH2-modified column. After remaining at room temperature for 24 h, the column was washed with toluene and methanol to give the Crn-PFPA column (see Scheme 1b). A control was prepared by charging the NH<sub>2</sub>modified silica monolith with PFPA-NHS in toluene (1.0 mg mL<sup>-1</sup>) at room temperature for 24 h and washing with toluene and methanol to give the PFPA column. Additionally, C60 column and C70 column were prepared following the protocols in our previous reports. The detailed preparation procedures are described in Supporting Information, Scheme

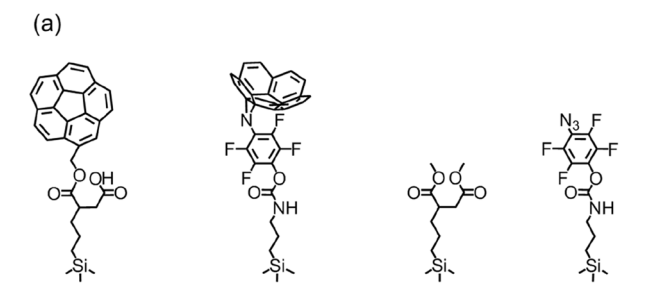
## ■ RESULTS AND DISCUSSION

**Preparation of Crn-Modified Silica Monoliths.** Two types of Crn derivatives were used to construct the columns: one was edge functionalized with hydroxymethyl (Crn-CH<sub>2</sub>OH) and the other was functionalized PFPA-NHS (Crn-PFPA-NHS) (Scheme 1). Crn-CH<sub>2</sub>OH was synthesized by first reacting Crn with an excess amount of dichloromethyl methyl ether in the presence of TiCl<sub>4</sub> at room temperature for 24 h to give the aldehyde derivative Crn-CHO, which was then reduced with NaBH<sub>4</sub> to give Crn-CH<sub>2</sub>OH in an overall 51% yield.<sup>37</sup>

PFPA-derivatized Crn, Crn-PFPA-NHS, was synthesized by heating Crn with PFPA-NHS in chlorobenzene at 108 °C for 5 days. PFPA undergoes cycloaddition with double bonds to form aziridine structures. Perfluorination of phenyl azide lowers the LUMO of the azide, facilitating its reaction with dipolarophiles and electrophiles.<sup>39</sup> PFPAs have also demonstrated good reactivity toward carbon materials such as fullerenes, 30,40 carbon nanotubes, 41 and graphene, 42-44 which are otherwise quite inert chemically. There are four types of double bonds in Crn, and therefore four different products are possible from the reaction with PFPA (Supporting Information, Figure S9). To facilitate structure determination of the product, a PFPA methyl ester, PFPA-CO<sub>2</sub>CH<sub>3</sub>, was used as a model compound for its simpler structure than PFPA-NHS. The aliphatic region of the <sup>1</sup>H NMR spectrum of the product only showed the methyl peak from PFPA-CO<sub>2</sub>CH<sub>3</sub>, thus ruling out the arizidine products from the addition to the flank and rim of Crn (B and D, Supporting Information, Figure S9) because these products include aliphatic CH moiety. The <sup>1</sup>H NMR spectrum of the product showed the peak patterns in the

aromatic region (Supporting Information, Figure S7). Computation of the orbital energies of PFPA and Crn supports the reaction between the LUMO of the azide in PFPA and the HOMO (Supporting Information, Figures S10 and S11). Results of the stabilization energy computed from the Hartree–Fock (HF) method (Supporting Information, Table S1) for structures A and C indicated that the most stable structure is structure A, which is consistent with our experimental data.

These Crn derivatives were then conjugated to a  $\rm CO_2H$ - or  $\rm NH_2$ -functionalized silica monolith by esterification or amidation to give the Crn-ester column and Crn-PFPA column, respectively (Scheme 1, and Supporting Information, Scheme S1). Columns that were modified with only the linkers, ester column, and PFPA column were also prepared and used as controls. Figure 1a shows the surface structure of the stationary phase in Crn-ester column, Crn-PFPA column, ester column, and PFPA column.



Crn-ester column Crn-PFPA column Ester column PFPA column

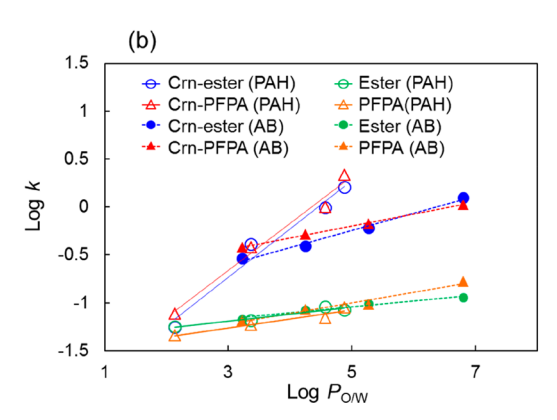


**Figure 1.** (a) Surface structure of the stationary phase in Crn-ester column, Crn-PFPA column, and the controls, ester column and PFPA column. (b) Log k vs Log  $P_{\text{o/w}}$  in each column. Condition: Crn-ester column (32.0 cm × 100  $\mu$ m i.d.), Crn-PFPA column (32.0 cm × 100  $\mu$ m i.d.), ester column (32.0 cm × 100  $\mu$ m i.d.), PFPA column (32.0 cm × 100  $\mu$ m i.d.); flow rate, 2.0  $\mu$ L min<sup>-1</sup>; mobile phase, water/methanol = 1/9; detection, UV 254 nm; temperature, 40 °C.

Figure 1b plots the retention factor k ( $k = (t_R - t_0/t_0; t_{R})$  retention time of a solute;  $t_0$ , elution time of nonretained solute (acetone)) of different alkylbenzenes (ABs) and PAH in these columns vs the water/octanol partition coefficient (Log  $P_{O/W}$ ), which indicates the hydrophobicity of the molecule. When the columns were modified with Crn (i.e., Crn-ester and Crn-PFPA columns), they showed stronger retention of ABs than other columns. Log k increased linearly with Log  $P_{O/W}$ . Additionally, Crn-ester column and Crn-PFPA column showed stronger retention for hydrophobic PAHs, while this was not observed on the control columns (ester and PFPA columns)

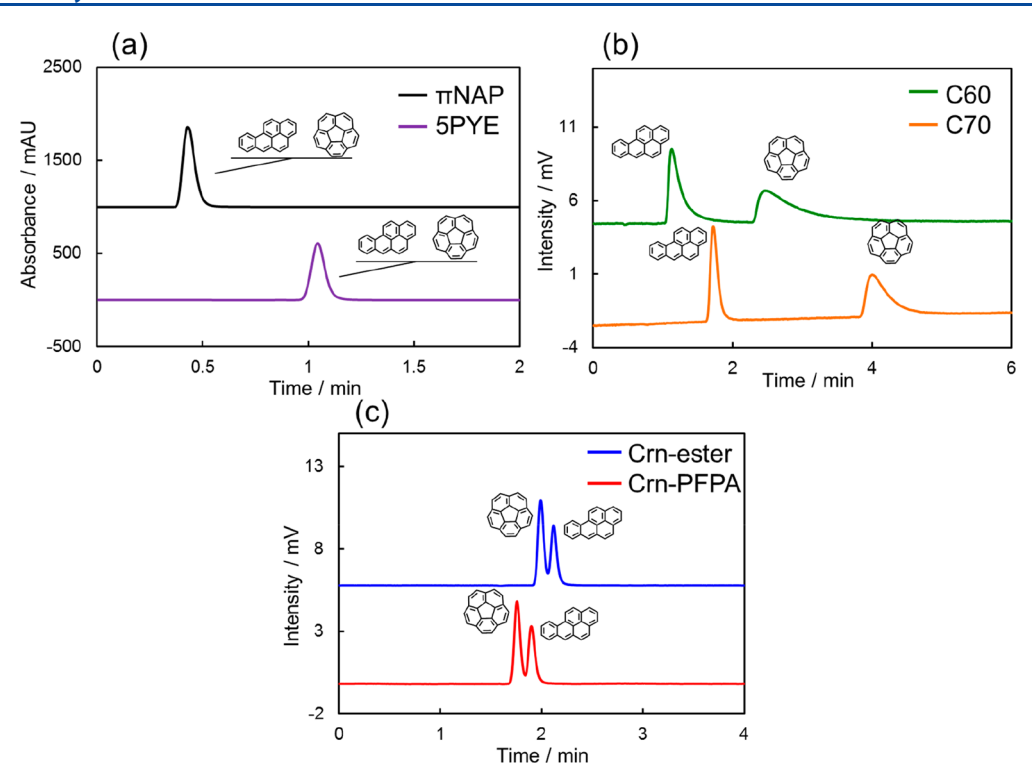


Figure 2. Chromatograms of the mixed sample of Crn and benzo [a] pyrene on (a)  $\pi$ NAP (Nacalai Tesque, 50 mm × 2.0 mm i.d.), 5PYE (Nacalai Tesque, 150 mm × 4.6 mm i.d.); (b) C60 column (32.0 cm × 100  $\mu$ m i.d.), C70 column (32.0 cm × 100  $\mu$ m i.d.); (c) Crn-ester column (32.0 cm × 100  $\mu$ m i.d.), Crn-PFPA column (32.0 cm × 100  $\mu$ m i.d.). Condition: flow rate, (a) 2.0 mL min<sup>-1</sup>, (b,c) 2.0  $\mu$ L min<sup>-1</sup>; mobile phase, chloroform/n-hexane = 3/7; detection, UV 254 nm; temperature, 40 °C.

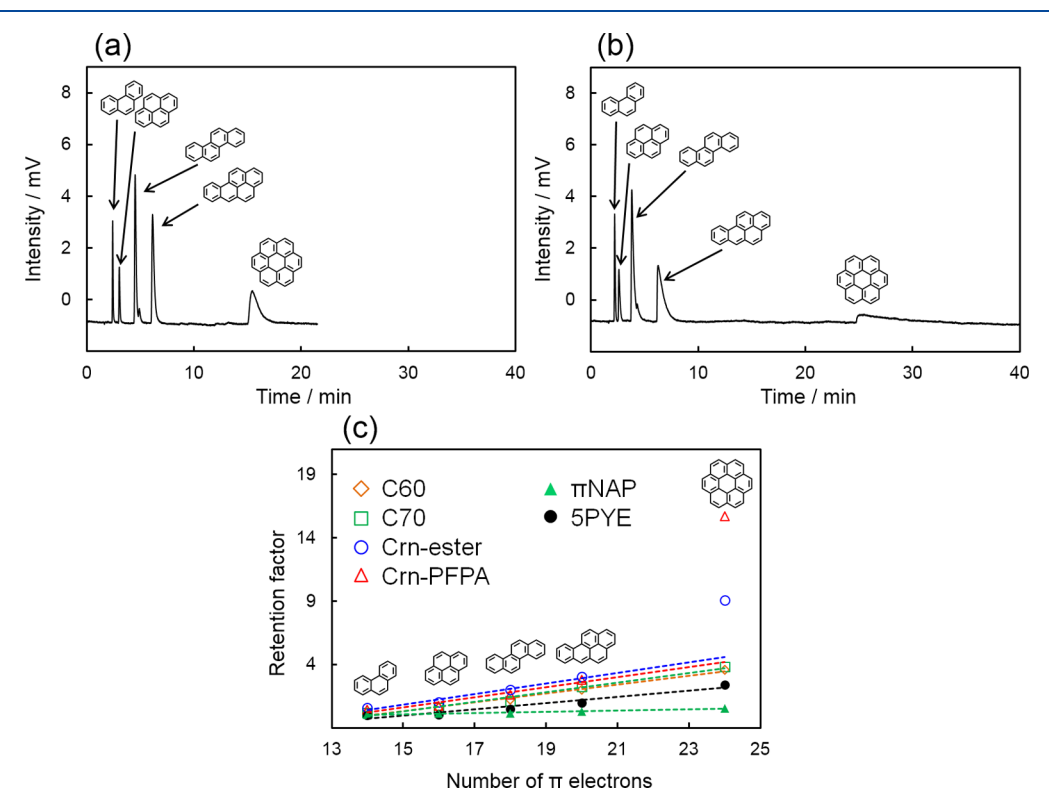


Figure 3. Retention behaviors of nonpolar and planar PAHs in Crn-modified silica monoliths. Chromatograms of the mixed sample of PAHs on (a) Crn-ester column and (b) Crn-PFPA column. (c) Plots of retention factor on each column vs the number of  $\pi$  electrons in PAH. Conditions: column, C60 column (32.0 cm × 100  $\mu$ m i.d.), C70 column (32.0 cm × 100  $\mu$ m i.d.), Crn-ester column (32.0 cm × 100  $\mu$ m i.d.),  $\pi$ NAP (Nacalai Tesque, 50 mm × 2.0 mm i.d.), and 5PYE (Nacalai Tesque, 150 mm × 4.6 mm i.d.); mobile phase, n-hexane; detection, UV 300 nm; temperature, 40 °C.

that were not modified with Crn. The results confirmed the existence of the hydrophobic interaction and  $\pi$  interaction derived from the Crn structure. Furthermore, these results clearly demonstrated the successful immobilization of Crn on Crn-ester and Crn-PFPA columns.

Retention Selectivity for Hemispherical Structure. In our previous reports, C60 and C70 showed higher recognition for Crn than typical planar PAH structures owing to the specific  $\pi$ – $\pi$  interaction between the spherical  $\pi$ -conjugated surfaces. <sup>31,32</sup> We expect that Crn-modified silica monoliths should show similarly spherical recognition owing to the hemispherical structure of Crn. To test the hypothesis, we included benzo[a]pyrene, which has the same number of  $\pi$  electrons as Crn but has a planar structure rather than the hemispherical structure in Crn, and evaluated the elution behavior of Crn and benzo[a]pyrene using Crn modified silica monoliths. For a comparison, C60 and C70 columns and commercially available LC columns that are known for their effective  $\pi$  interaction (PYE and  $\pi$ NAP (Nacalai Tesque, Kyoto, Japan)) were tested under the same conditions.

Chromatograms of the mixed sample of Crn and benzo [a]pyrene on each column are shown in Figure 2. On the commercially LC columns PYE and  $\pi$ NAP, there were no differences in the strength of  $\pi$  interactions between Crn and benzo[a]pyrene, likely due to the small-planar  $\pi$ -conjugated structure that are used to modify the columns (Figure 2a). On the other hand, fullerene-modified silica monoliths showed stronger retention for Crn than that of benzo[a]pyrene, which can be attributed to spherical recognition (Figure 2b). Surprisingly, Crn-modified silica monoliths showed lower retentions for Crn than benzo[a]pyrene (Figure 2c). This result implies a significantly lower interaction between Crn structures themselves than their interaction with fullerene. In our earlier study, we confirmed that the effective retention of Crn on C70 column was caused by the dipole of Crn inducing dipoles in C70. Hence, we hypothesize that the repulsion between the hemispherical structures of Crn is caused by the dipole moment.

A computational study was carried out in order to understand the charge state of each carbon atom on Crn and Crn derivatives. The detailed calculation conditions are described in the Supporting Information. Figure 3 shows the charge on each carbon atom and the charge distribution in Crn and Crn derivatives. The carbon atoms in Crn exhibited alternating negative and positive charges (Supporting Information, Figure S12b,c). Crn derivatives exhibited similar trend, with the exception of those carbon atoms that were functionalized (C3, and to a lesser extent C2 and C4 in Crn-CH<sub>2</sub>OH; C1 and C2, and to a lesser extent C3 and C4 in Crn-PFPA, Supporting Information, Figure S12b). As such, if Crn in the mobile phase overlaps with the Crn structure on the stationary phase, electrostatic repulsions would occur between their dipole moments. In this case, Crn-modified silica monoliths would not be able to interact with Crn in the mobile phase due to the electrostatic repulsion resulting from the same arrangements of atomic charges in the Crn structures. Even in the Crn-ester column, in which both concave and convex surfaces of the Crn structure could interact with Crn, the repulsion effect was observed. A similar result was reported by Wang et al. that neighboring Crn structures were not completely stacked in the crystal structure, which is consistent with our observation.<sup>45</sup>

On the basis of the above results, we hypothesize that intramolecular dipoles in aromatic compounds could decrease the strength of  $\pi$ - $\pi$  interactions with other polar aromatic compounds resulting from charge repulsion. To test this, we evaluated separation behaviors between the nonpolar naphthalene and the polar azulene, 46 both of which are of planar structures and have the identical number of  $\pi$  electrons. As shown in Supporting Information, Figure S13, We found that Crn-modified silica monoliths showed weaker retention and lower selectivity to azulene than the fullerene-modified columns. On the other hand, Crn-modified silica monoliths exhibited stronger retentions than fullerene-modified columns for naphthalene due to intramolecular dipoles in Crn structures and induced dipole in naphthalene. Thus, we suggest that polar aromatic compounds showed lower affinity to other polar aromatic compounds than nonpolar compounds regardless of plane or curved structures.

Retention Behaviors of PAHs with Different  $\pi$ Electron Numbers. In the last section, we clarified the interaction of Crn with polar aromatic compounds and elucidated the retention behavior based on the nature of charge interactions. In this section, we evaluate the retention selectivity of nonpolar and planar PAHs in Crn-modified silica monoliths. The typical chromatograms obtained by normal phase mode of PAHs, including phenanthrene, pyrene, chrysene, benzo[a]pyrene, and coronene are shown in Figure 3a,b). Both Crn-ester and Crn-PFPA columns strongly retained PAHs. The retention increased with the number of  $\pi$  electrons and showed high separation resolution owing to the strong  $\pi - \pi$  interaction. To demonstrate the retention selectivity in the Crn-modified silica monoliths, the retention factor for each PAH is plotted against the number of  $\pi$ electrons. As shown in Figure 3c, PAHs were retained in Crn columns slightly better than other columns, which can be attributed to the dipole of Crn. Interestingly, in both Crn-ester and Crn-PFPA columns, coronene was significantly retained compared to other planar PAHs, whereas a linear relation was observed for all the PAHs in the C60, C70 (Supporting Information, Scheme S2), PYE, and  $\pi$ NAP columns. Especially, the retention of coronene was much higher in Crn-PFPA column than in Crn-ester column. In Crn-PFPA, because PFPA derivatization occurs on the spoke of Crn (Scheme 1), only the concave surface of Crn structure in the Crn-PFPA column could interact with coronene because of the large steric hindrance of nitrogen atom on the concave surface. In the Crn-ester column, however, because the derivatization occurs at the edge of the structure, both concave and convex surfaces of the Crn structure could interact with coronene.

To elucidate the additional intramolecular interactions between coronene and Crn structures, the <sup>1</sup>H NMR spectra of Crn-CH<sub>2</sub>OH or Crn-PFPA-CH<sub>2</sub>OCH<sub>3</sub> in the presence of coronene were recorded and compared to those of coronene or the Crn derivatives. No significant peak shifts were observed in either coronene or Crn-CH<sub>2</sub>OH when the two molecules were mixed (Supporting Information, Figure S14a). However, when coronene was mixed with Crn-PFPA-CH<sub>2</sub>OCH<sub>3</sub>, the aromatic peaks in Crn-PFPA-CH<sub>2</sub>OCH<sub>3</sub> shifted upfield and the width of several peaks were also broadened, while no shift was observed for the methyl protons.

In general,  $\pi$  interactions can be interfered with by polar molecules such as halogenated compounds, thus the interaction between Crn and coronene may not be fairly evaluated in chloroform. In fact, the retentions due to  $\pi$ 

interactions were dramatically decreased by adding chloroform to the mobile phase in LC. Therefore, to better evaluate the chemical shifts in NMR, we added n-hexane- $d_{14}$  to chloroform-d because  $\pi$  interactions appear more strongly in n-hexane, due to its lower dielectric constant, than in chloroform. As expected, significant shifts of the aromatic protons in both coronene and Crn-PFPA-CH<sub>2</sub>OCH<sub>3</sub> were observed in n-hexane- $d_{14}$ /chloroform-d. As shown in Figure 4, the aromatic

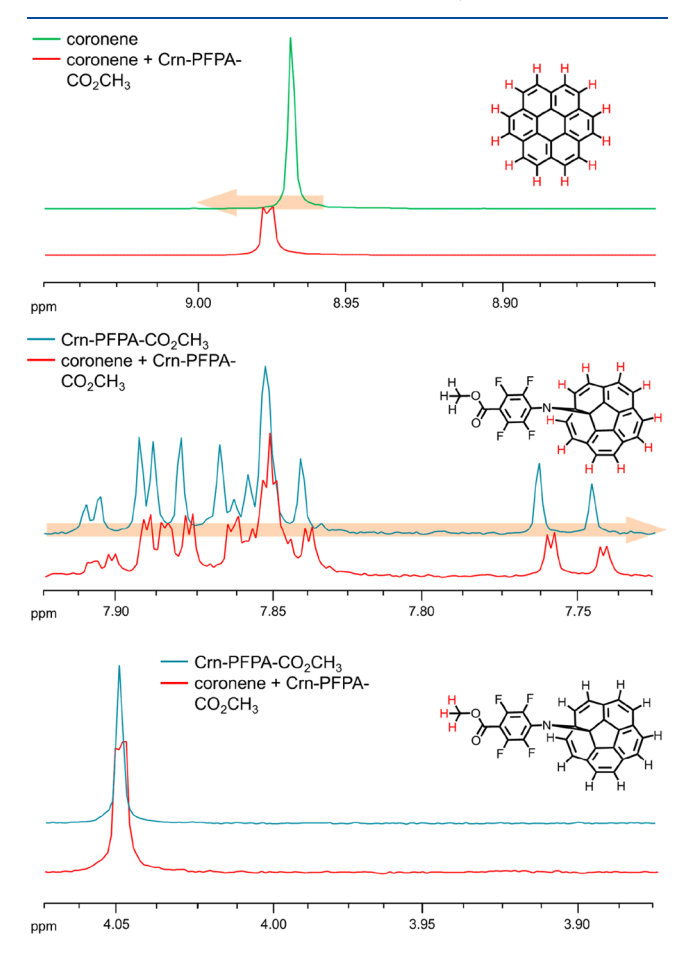


**Figure 4.** <sup>1</sup>H NMR spectral comparisons of coronene, Crn-PFPA-CH<sub>2</sub>OCH<sub>3</sub>, or their mixture in hexane- $d_{14}$ /chloroform-d = 1/1.

peak in coronene shifted downfield after mixing with Crn-PFPA-CH<sub>2</sub>OCH<sub>3</sub>, whereas all Crn aromatic protons in Crn-PFPA-OCH<sub>3</sub> shifted upfield. In addition, these peaks were bifurcated and broadened. These drastic changes suggest the presence of extremely strong intermolecular interactions. Thus, the protons on the Crn structure were placed in a more electron rich environment (more shielded), whereas the protons on coronene were placed in a more electron poor environment (less shielded). In other words, as the Crn structure approached the  $\pi$  conjugated surface of coronene, it attracted the  $\pi$  electrons in coronene, making its aromatic protons more shielded.

This is likely mediated by the strong electron-withdrawing PFPA on Crn-PFPA-CH<sub>2</sub>OCH<sub>3</sub>, which pulls the electron density away from Crn and, subsequently, coronene. Briefly, strong CH $-\pi$  interaction at multiple points working between the hydrogen atom of Crn and the aromatic ring of coronene was confirmed. Matsuno et al. recently reported multipoint and strong  $\pi$  interaction between (P)-(12,8)-[4] cyclo-2,8-chrys-

enylene, which is a cylindrical molecule made of linked chrysen structure in a hoop-like structure, and Crn. Our results are also strongly supported from this report.<sup>48</sup>

Figure 5 shows a schematic diagram illustrating the  $\pi$  interaction of coronene with Crn in Crn-ester or Crn-PFAP

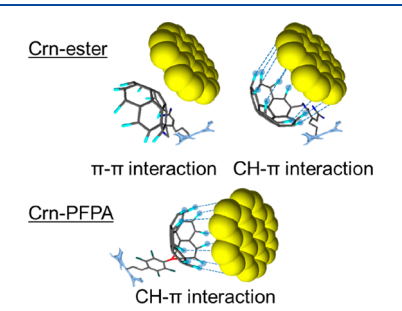


**Figure 5.** Schematic diagram of  $\pi$  interaction between coronene and Crn in Crn-ester or Crn-PFPA column.

column. On the Crn-ester column, Crn was edge-functionalized and the linker is away from the Crn surface. As such, both concave and the convex surfaces of Crn can interact with coronene. On the Crn-PFPA column, because the modification by PFPA occurs on the spoke of Crn, the strong steric hindrance puts the PFPA group on the convex surface of the Crn structure. This leaves mainly the concave surface of Crn to interact with coronene. The fact that the Crn-PFPA column had significantly higher retention for coronene than the Crnester column demonstrates that the CH- $\pi$  interaction on this concave surface is much stronger than the interaction from both surfaces in Crn-ester.

**Shape Recognition.** We show in last section that both convex and concave surfaces of the Crn structure contributed to the molecular recognition in the Crn-ester column, while only the concave surface of the Crn structure contributed in the Crn-PFPA column. To investigate whether the shape recognition plays a role, we evaluated the retention selectivity of naphthacene and triphenylene, which are planar aromatic compounds that have the same number of  $\pi$  electrons, and the only difference is the molecular shape. The chromatograms obtained by normal phase mode of naphthacene and triphenylene are shown in Figure 6. Interestingly, the elution order was reversed; triphenylene eluted faster than naphthacene on the Crn-PFPA column, while the opposed result was obtained on the Crn-ester column.

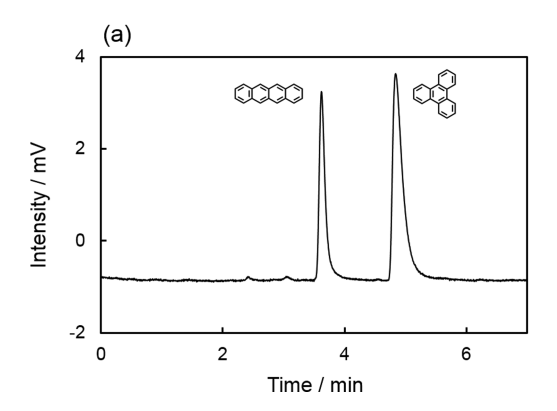
To investigate the difference in shape recognition, we consider the difference in the polarizability of these PAHs. In the case of nonpolar molecules in  $\pi$  interaction, the strength of  $\pi$  interaction is considered to be due to induced dipole—dipole interaction or induced dipole—induced dipole interaction. The potential energy of induced dipole—induced dipole interaction is given as follows:

$$G_{\rm induced-dipole-dipole} = -\mu^2 \alpha_1/(4\pi\varepsilon_0 \varepsilon_r)^2 r^6 \tag{1}$$

The potential energy of induced dipole—dipole interaction is given as follows:

$$G_{\text{induced-dipole}-\text{induced-dipole}} = -A\alpha_1\alpha_2/(4\pi\varepsilon_0\varepsilon_r)^2r^6$$
 (2)

where A is a constant depending on the ionization energy,  $\mu$  is the dipole moment of polar molecules,  $\alpha$  are polarizabilities of the molecules,  $\varepsilon_0$  is the permittivity of vacuum,  $\varepsilon_r$  is the permittivity of the solvent, and r is the distance between the



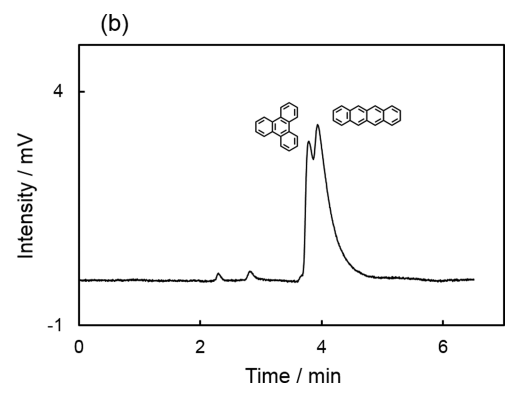


Figure 6. Chromatograms of the mixed sample of naphthacene and triphenylene on (a) Crn-ester column and (b) Crn-PFPA column. Condition: column, Crn-ester column (32.0 cm  $\times$  100  $\mu$ m i.d.), Crn-PFPA column (32.0 cm  $\times$  100  $\mu$ m i.d.); mobile phase, n-hexane; detection, UV 280 nm; temperature, 40 °C.

molecules, respectively.  $^{51,52}$  In this case, the strength of  $\pi$  interaction increases as the polarizability of the solute increases.

Then, we consider that the difference in shape recognition was caused by the polarizability of these PAHs. The polarizability of PAHs was summarized in Supporting Information, Table S2, and the polarizability is plotted against the number of  $\pi$  electrons (Supporting Information, Figure S15). As shown in Supporting Information, Figure S15, the polarizability of each solute increases roughly with the number of  $\pi$  electrons. This trend is consistent with increasing in retention and the stronger  $\pi$  interaction as the number of  $\pi$ electrons increases. For those PAHs with identical number of  $\pi$ electrons, small differences in the polarizability were observed, e.g., naphthacene, benzo[a]anthracene, chrysene, and triphenylene. As further examination regarding the shape recognition (Supporting Information, Figure S16), the convex surface of Crn contributes to retention in the Crn-ester column in contrast to the Crn-PFPA column that the concave surface contributed to the retention. In summary, the concave surface of Crn in Crn-PFPA column dominated the interactions with the solutes.

#### CONCLUSIONS

In this report, we revealed the molecular recognition of Crn by evaluating the retention of Crn as well as a number of aromatic compounds on Crn-modified silica monoliths in LC. We synthesized two kinds of Crn derivatives, Crn-ester by introducing the functional group on the edge of Crn, and Crn-PFPA by modifying the spoke structure of corannulene, and successfully prepared the Crn-modified columns Crn-ester and Crn-PFPA. Both columns showed low retention for Crn despite its hemispherical structure. Computer simulation of Crn and Crn derivatives suggested electrostatic repulsion resulting from the same arrangements of charge and charge distributions in the Crn structures. On the other hand, both columns exhibited strong interactions with the planar molecule, coronene, especially Crn-PFPA, which showed significantly strong interactions. The evaluation of <sup>1</sup>H NMR shifts suggested that the specific retention was caused by  $CH-\pi$  interaction at multiple points between the hydrogen atoms of the concave surface of Crn structure and the planar  $\pi$ conjugated surface of coronene. Furthermore, we demonstrated that the molecular recognition in Crn-ester was due to  $\pi$ - $\pi$  interaction on the convex surface of Crn. We believe that

this report greatly advanced our understanding on the  $\pi$  interactions, which should aid the development of novel functional materials.

### ASSOCIATED CONTENT

## **S** Supporting Information

The Supporting Information is available free of charge on the ACS Publications website at DOI: 10.1021/acs.analchem.8b05260.

Detailed experimental procedures, synthesis of 4-azido-2,3,5,6-tetrafluorophenyl succinate (PFPA-NHS), preparation of a silica-monolithic capillary, computational methods, structure of PAHs, synthesis of Crn-CH<sub>2</sub>OH, synthesis of Crn-PFPA-CO<sub>2</sub>CH<sub>3</sub>, calculations for the reaction between PFPA and Crn, and preparation of C60/C70 columns (PDF)

## AUTHOR INFORMATION

## **Corresponding Author**

\*Tel: +81-75-383-2448. Fax: +81-75-383-2450. E-mail: kubo@anchem.mc.kyoto-u.ac.jp.

# ORCID ®

Takuya Kubo: 0000-0002-9274-3295 Mingdi Yan: 0000-0003-1121-4007

#### Notes

The authors declare no competing financial interest.

#### ACKNOWLEDGMENTS

This research was partly supported by the Grant-in Aid for Scientific Research (no. 25620111 and 15K13756) from the Japan Society for the Promotion of Science, an Environment Research and Technology Development Fund (5-1552) from the Ministry of the Environment, Japan. M.Y. thanks the financial support from the National Science Foundation (CHE-1112436, CHE-1808671).

## REFERENCES

- (1) Cornil, B. J.; Beljonne, D.; Calbert, J.; Brédas, J. Adv. Mater. **2001**, 13, 1053-1067.
- (2) Mignon, P.; Loverix, S.; Steyaert, J.; Geerlings, P. Nucleic Acids Res. 2005, 33, 1779–1789.
- (3) Wilson, K. A.; Kellie, J. L.; Wetmore, S. D. Nucleic Acids Res. **2014**, 42, 6726–6741.
- (4) Salonen, L. M.; Ellermann, M.; Diederich, F. Angew. Chem., Int. Ed. 2011, 50, 4808–4842.

- (5) Neel, A. J.; Hilton, M. J.; Sigman, M. S.; Toste, F. D. Nature 2017, 543, 637-646.
- (6) Nakagawa, Y.; Irie, K.; Yanagita, R. C.; Ohigashi, H.; Tsuda, K. I. *I. Am. Chem. Soc.* **2005**, *127*, 5746–5747.
- (7) Okamoto, T.; Nakahara, K.; Saeki, A.; Seki, S.; Oh, J. H.; Akkerman, H. B.; Bao, Z.; Matsuo, Y. Chem. Mater. **2011**, 23, 1646–1649.
- (8) Wu, H.; Zhao, P.; Li, X.; Chen, W.; Ågren, H.; Zhang, Q.; Zhu, L. ACS Appl. Mater. Interfaces 2017, 9, 3865–3872.
- (9) Barth, W. E.; Lawton, R. G. J. Am. Chem. Soc. 1966, 88, 380-381.
- (10) Olson, A. J.; Hu, Y. H. E.; Keinan, E. Proc. Natl. Acad. Sci. U. S. A. 2007, 104, 20731–20736.
- (11) Lovas, F. J.; McMahon, R. J.; Grabow, J. U.; Schnell, M.; Mack, J.; Scott, L. T.; Kuczkowski, R. L. *J. Am. Chem. Soc.* **2005**, 127, 4345–4349.
- (12) Wang, L.; Wang, W. Y.; Qiu, Y. Q.; Lu, H. Z. J. J. Phys. Chem. C **2015**, 119, 24965–24975.
- (13) Lu, R. Q.; Xuan, W.; Zheng, Y. Q.; Zhou, Y. N.; Yan, X. Y.; Dou, J. H.; Chen, R.; Pei, J.; Weng, W.; Cao, X. Y. A RSC Adv. 2014, 4. 56749–56755.
- (14) Hashemi, M. M.; Bratcher, M. S.; Scott, L. T. J. J. Am. Chem. Soc. 1992, 114, 1920-1921.
- (15) Juríček, M.; Strutt, N. L.; Barnes, J. C.; Butterfield, A. M.; Dale, E. J.; Baldridge, K. K.; Stoddart, J. F.; Siegel, J. S. *Nat. Chem.* **2014**, *6*, 222–228.
- (16) Kawasumi, K.; Zhang, Q.; Segawa, Y.; Scott, L. T.; Itami, K. Nat. Chem. 2013, 5, 739–744.
- (17) Mishra, A.; Ulaganathan, M.; Edison, E.; Borah, P.; Mishra, A.; Sreejith, S.; Madhavi, S.; Stuparu, M. C. ACS Macro Lett. 2017, 6, 1212–1216.
- (18) Sygula, A.; Fronczek, F. R.; Sygula, R.; Rabideau, P. W.; Olmstead, M. M. J. Am. Chem. Soc. 2007, 129, 3842-3843.
- (19) Mack, J.; Vogel, P.; Jones, D.; Kaval, N.; Sutton, A. Org. Biomol. Chem. 2007, 5, 2448–2452.
- (20) Wells, R. A.; Kellie, J. L.; Wetmore, S. D. J. Phys. Chem. B **2013**, 117, 10462–10474.
- (21) Tsuzuki, S.; Honda, K.; Uchimaru, T.; Mikami, M.; Tanabe, K. J. Am. Chem. Soc. **2000**, 122, 11450–11458.
- (22) Huber, R. G.; Margreiter, M. A.; Fuchs, J. E.; Von Grafenstein, S.; Tautermann, C. S.; Liedl, K. R.; Fox, T. J. Chem. Inf. Model. 2014, 54, 1371–1379.
- (23) Kawahara, S. I.; Tsuzuki, S.; Uchimaru, T. J. Chem. Phys. 2003, 119, 10081–10087.
- (24) Kohn, S. C.; Dupree, R.; Smith, M. E. Nature 1989, 337, 539–541.
- (25) Ramírez-Gualito, K.; Alonso-Ríos, R.; Quiroz-García, B.; Rojas-Aguilar, A.; Díaz, D.; Jiménez-Barbero, J.; Cuevas, G. *J. Am. Chem. Soc.* **2009**, *131*, 18129–18138.
- (26) Li, P.; Zhao, C.; Smith, M. D.; Shimizu, K. D. J. Org. Chem. **2013**, 78, 5303–5313.
- (27) Del Bene, J. E.; Perera, S. A.; Bartlett, R. J. J. Phys. Chem. A 1999, 103, 8121-8124.
- (28) Kimata, K.; Hosoya, K.; Araki, T.; Tanaka, N. J. Org. Chem. 1993, 58, 282–283.
- (29) Chen, S.; Meyerhoff, M. Anal. Chem. 1998, 70, 2523-2529.
- (30) Kubo, T.; Murakami, Y.; Tominaga, Y.; Naito, T.; Sueyoshi, K.; Yan, M.; Otsuka, K. *J. Chromatogr. A* **2014**, *1323*, 174–178.
- (31) Kubo, T.; Murakami, Y.; Tsuzuki, M.; Kobayashi, H.; Naito, T.; Sano, T.; Yan, M.; Otsuka, K. *Chem. Eur. J.* **2015**, *21*, 18095–18098.
- (32) Kubo, T.; Kanao, E.; Matsumoto, T.; Naito, T.; Sano, T.; Yan, M.; Otsuka, K. ChemistrySelect 2016, 1, 5900–5904.
- (33) Kanao, E.; Kubo, T.; Naito, T.; Matsumoto, T.; Sano, T.; Yan, M.; Otsuka, K. J. Phys. Chem. C 2018, 122, 15026–15032.
- (34) Kanao, E.; Naito, T.; Kubo, T.; Otsuka, K. Chromatography 2017, 38, 45-51.
- (35) Mizyed, S.; Georghiou, P. E.; Bancu, M.; Cuadra, B.; Rai, A. K.; Cheng, P.; Scott, L. T. *J. Am. Chem. Soc.* **2001**, *123*, 12770–12774.

- (36) Li, J.; Liu, Y.; Qian, Y.; Li, L.; Xie, L.; Shang, J.; Yu, T.; Yi, M.; Huang, W. Phys. Chem. Chem. Phys. **2013**, 15, 12694–12701.
- (37) Rajeshkumar, V.; Lee, Y. T.; Stuparu, M. C. Eur. J. Org. Chem. **2016**, 2016, 36-40.
- (38) Liu, L.-H.; Yan, M. Acc. Chem. Res. 2010, 43, 1434-1443.
- (39) Xie, S.; Lopez, S. A.; Ramström, O.; Yan, M.; Houk, K. N. J. Am. Chem. Soc. 2015, 137, 2958–2966.
- (40) Yan, M.; Cai, S. X.; Keana, J. F. W. J. Org. Chem. 1994, 59, 5951-5954.
- (41) Kong, N.; Shimpi, M. R.; Park, J. H.; Ramström, O.; Yan, M. Carbohydr. Res. **2015**, 405, 33–38.
- (42) Park, J.; Yan, M. Acc. Chem. Res. 2013, 46, 181-189.
- (43) Park, J.; Jayawardena, H. S.; Chen, X.; Jayawardana, K. W.; Sundhoro, M.; Ada, E.; Yan, M. Chem. Commun. 2015, 51, 2882–2885
- (44) Park, J.; Jin, T.; Liu, C.; Li, G.; Yan, M. ACS Omega 2016, 1, 351-356.
- (45) Wang, B. T.; Petrukhina, M. A.; Margine, E. R. Carbon 2015, 94, 174-180.
- (46) Grimme, S. Chem. Phys. Lett. 1993, 201, 67-74.
- (47) Jennings, W. B.; McCarthy, N. J. P.; Kelly, P.; Malone, J. F. Org. Biomol. Chem. **2009**, *7*, 5156–5162.
- (48) Matsuno, T.; Fujita, M.; Fukunaga, K.; Sato, S.; Isobe, H. Nat. Commun. 2018, 9, 3779.
- (49) Lima, C. F. R. A. C.; Rocha, M. A. A.; Gomes, L. R.; Low, J. N.; Silva, A. M. S.; Santos, L. M. N. B. F. *Chem. Eur. J.* **2012**, *18*, 8934–8943.
- (50) Wagner, J. P.; Schreiner, P. R. Angew. Chem., Int. Ed. 2015, 54, 12274–12296.
- (51) Liang, Y. Q.; Hunt, K. L. C. J. Chem. Phys. 1993, 98, 4626-4635.
- (52) Bowen, W. R.; Jenner, F. Adv. Colloid Interface Sci. 1995, 56, 201–243.